NASA TECHNICAL REPORT

NASA TR R-206

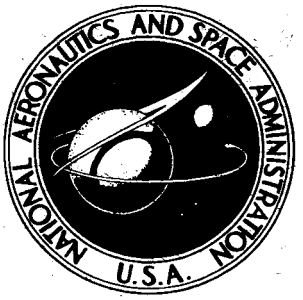

NASA TR R-206

ON THE STABILITY OF THE BOUNDARY OF THE GEOMAGNETIC FIELD

by John R. Spreiter and Audrey L. Summers

Ames Research Center

Moffett Field, Calif.

NATIONAL AERONAUTICS AND SPACE ADMINISTRATION • WASHINGTON, D. C. • MAY 1965

ON THE STABILITY OF THE BOUNDARY OF THE GEOMAGNETIC FIELD

By John R. Spreiter and Audrey L. Summers

Ames Research Center
Moffett Field, Calif.

NATIONAL AERONAUTICS AND SPACE ADMINISTRATION

For sale by the Clearinghouse for Federal Scientific and Technical Information
Springfield, Virginia 22151 – Price $2.00

ON THE STABILITY OF THE BOUNDARY OF THE GEOMAGNETIC FIELD

By John R. Spreiter and Audrey L. Summers

Ames Research Center
Moffett Field, Calif.

SUMMARY

The response of the magnetosphere boundary in a steady solar wind to small initial departures from equilibrium is investigated in accordance with the classical model of Chapman and Ferraro. If the wavelength and amplitude are sufficiently small that curvature and second-order effects can be disregarded, all perturbations, except those having wave fronts alined with the direction of the local magnetic field, are found to damp exponentially with time and to drift along the boundary with the tangential component of the solar wind. Alined waves, which neither damp nor amplify in this approximation, are examined further by inclusion of curvature and higher order effects. A first-order analysis shows that curvature introduces a destabilizing effect in small regions in the vicinity of the neutral points and a stabilizing effect elsewhere. Possible geophysical consequences, such as the persistent magnetic agitation of the polar regions, are discussed. An exact solution for an alined cylindrical solitary wave having an initial form of a circular arc is also presented to illustrate a mode of response that appears to permit injection of elongated and widely separated columns of solar wind plasma into the magnetosphere under certain conditions and to provide a mechanism for momentum transfer from the solar wind to the ambient magnetosphere plasma.

INTRODUCTION

This paper is concerned with a theoretical determination of the dynamical response of the boundary of the geomagnetic field in a steady solar wind to a small initial disturbance from the equilibrium configuration. It differs from previous related studies by Dungey (refs. 1 and 2) and Parker (ref. 3) in that (a) the analysis is based on strict application of the classical theory of Chapman and Ferraro and does not invoke additional assumptions, such as those brought over from the study of somewhat analogous hydrodynamic problems related to the generation of surface waves by wind, and (b) effects of nonlinear terms and of curvature of the equilibrium shape of the boundary are included in those cases that are neutrally stable in the first approximation.

Although the Chapman-Ferraro theory is itself a highly simplified theory, it has emerged from numerous comparisons with experiments conducted in space as the leading theory for explaining many features of the interaction between the geomagnetic field and the solar wind. It is true that such comparisons

and other considerations have shown that additional features, such as a detached bow wave or viscous or turbulent mixing at the boundary, are probably important, but they appear more as additions than alterations to the basic theory (e.g., see refs. 4 and 5 for recent résumés). Inasmuch as the present application of the Chapman-Ferraro theory is intermediate between the two principal previous applications to the interaction of the geomagnetic field with a steady solar wind and with the front of an immense and rapidly advancing cloud of solar plasma (see ref. 6 for an extensive review of these applications), it is anticipated that the results will have the same general degree of validity and usefulness. At very least, the results have merit in their own right as part of a consistent set of formal deductions and consequences of the basic Chapman-Ferraro model of the interaction of the geomagnetic field and solar plasma.

The results themselves have a number of features in common with those given previously by Dungey and Parker, and some features that differ substantially therefrom. In particular, the conclusion that the boundary of the geomagnetic field is unstable is not supported in general by the present results. The results thus appear to be more in keeping with the suggestion of Dessler (refs. 7 and 8) that magnetometer and plasma data indicate the boundary to be stable. (See, however, ref. 9 for a commentary on the earlier of these papers.) In some respects, however, the dynamical response determined in the present analysis is more complicated than can be described by a simple statement of stability or instability. It is found, for instance, that a small portion of the boundary over the polar regions is always unstable for a certain class of initial disturbances. A major portion of the boundary, however, is stable to sufficiently small disturbances, although unstable to larger disturbances. The analysis also discloses a mode of response that appears to permit injection of elongated and widely spaced columns of solar plasma into the magnetosphere under certain conditions and to provide a mechanism for momentum transfer from the solar wind to the plasma contained in the magnetosphere.

A somewhat similar injection mechanism has also been proposed recently by Barthel and Sowle (ref. 10). Details of the analysis are different in several respects, however, and the final conclusion differs in one very important feature. In particular, Barthel and Sowle conclude that injection will occur only if there is a very sudden increase in the intensity of the solar wind, such as might occur with a frequency of about 10 per year following large solar flares. The present analysis suggests, however, that injection will occur with even very modest irregularities in the solar wind, such as might be capable of forming an elongated dent in the magnetosphere boundary having an initial depth of only a few tens of kilometers.

STATEMENT OF MATHEMATICAL PROBLEM

The theory of Chapman and Ferraro provides a precise, although idealized, representation of the interaction between the geomagnetic field and the solar wind, be it steady or unsteady. According to this theory, the solar wind is considered to be free from significant influence of magnetic fields, and the

earth is considered to be devoid of any atmosphere in the region penetrated by the solar plasma. The interaction is such that a current system is established which terminates the geomagnetic field abruptly at a distance of the order of ten or more earth radii from the earth, and which leads to forces that retard and repel the advance of solar plasma toward the earth. In this way, the geomagnetic field is confined to a hollow or cavity carved out of the solar plasma. Within this cavity, or magnetosphere, the magnetic field satisfies the equations of a static magnetic field in a vacuum, that is

$$\text{div } \underset{\sim}{B} = 0 , \qquad \text{curl } \underset{\sim}{B} = 0 \tag{1}$$

The total magnetic field $\underset{\sim}{B}$ in the magnetosphere is the sum of the permanent magnetic field $\underset{\sim}{B}_p$ of the earth and induced magnetic fields $\underset{\sim}{B}'$ due to electric currents in the ionosphere, the magnetosphere, and at the interface between the magnetosphere and the solar wind. The permanent magnetic field is usually represented in studies of the boundary of the geomagnetic field by a simple magnetic dipole placed at the center of the earth and alined with the geomagnetic axis as determined from magnetic surveys. The effects of electric currents within the ionosphere and the magnetosphere are usually considered to be too small, and also too uncertainly known, to be included in the analysis, although the effects of the presence of a substantial ring current on the location of the boundary of the geomagnetic field in a steady solar wind have been investigated by Spreiter and Alksne (refs. 11 and 12). In this paper, we are concerned only with the dynamical response of an element of the boundary to a small initial displacement from its equilibrium location. For this purpose a detailed specification of magnetization and current distribution at points far removed from the element is not required.

A complete mathematical description does require, however, that appropriate conditions be specified at the boundary of the magnetosphere, that is, at the magnetopause. Since the location of the magnetopause is unknown and must be determined as part of the solution, it is necessary to specify two boundary conditions to determine a unique solution. One is that the normal component of the geomagnetic field vanish at the magnetopause, that is

$$\underset{\sim}{B}_s \cdot \hat{n}_s = B_n = 0 \tag{2}$$

where $\underset{\sim}{B}_s$ refers to the value of $\underset{\sim}{B}$ at the magnetopause and $\hat{n}_s$ refers to the unit normal taken positive when directed into the magnetosphere. The second is that the pressure exerted on the boundary by the particles of the solar wind be balanced by the magnetic pressure $B_s^2/8\pi$. This relation may be written as

$$B_s^2/8\pi = Kmn[(\underset{\sim}{V} - \underset{\sim}{v}) \cdot \hat{n}_s]^2 \tag{3}$$

where m, n, and $\underset{\sim}{V}$ refer to the mass, number density, and velocity of the ions (generally considered to be principally protons) of the undisturbed incident stream, $\underset{\sim}{v}$ refers to the local velocity of an element of the magnetopause, and K is a constant coefficient. It is required, in addition that

$$(\underset{\sim}{V} - \underset{\sim}{v}) \cdot \hat{n}_s \geq 0 \tag{4}$$

in order to avoid the occurrence of regions of the magnetopause that are shielded from direct impact by particles of the solar wind, and for which equation (3) would be inappropriate.

It has historically been considered that the particles are, in effect, specularly reflected at the boundary in which case $K = 2$ (see refs. 13 and 14 for a discussion of other values for K that have sometimes been used for this case). It has been argued recently by Axford (ref. 15), Kellogg (ref. 16), Spreiter and Jones (ref. 17), and others, however, that the presence of a weak interplanetary field may have the important effect of causing the solar wind to behave as a continuous fluid over length scales that are large compared with the proton Larmor radius. Since the Larmor radius is about 600 km for a 300 km/sec proton in a magnetic field of 5γ and a typical dimension of the magnetosphere is of the order of 10^5 km, it follows that the solar wind would flow around the magnetosphere much as a fluid about a solid object. Since, moreover, the effective Mach number based on the speed of a magnetoacoustic wave is much greater than unity, there would be a detached bow wave upstream from the magnetosphere. Nevertheless, the aerodynamic pressure exerted by the wind on the boundary would still be represented, according to the Newtonian theory of hypersonic flow, by the right side of equation (3) with $K = 1$. This change from $K = 2$ to $K = 1$, without further change of the governing equations (1) through (4), leaves the calculated form of the magnetopause unaltered, although all linear dimensions from the center of the earth to the magnetopause increased by a factor of $2^{1/6}$. Results so obtained have been shown (IG Bulletin 84, June 1964) to be in excellent agreement with data obtained in space with IMP-I satellite (Explorer XVIII). The effects of such a change are of even less importance in the present investigation, since we are concerned with deviations from the equilibrium configuration, and K cancels out of the analysis in most cases.

The equilibrium steady-state configuration of the magnetopause and the enclosed magnetic field is defined by the same set of equations, except that $\underset{\sim}{V}$ is equated to zero in equations (3) and (4). Equation (3) is thus replaced by

$$B_{se}^2/8\pi = Kmn(\underset{\sim}{V} \cdot \hat{n}_{se})^2 \qquad (5)$$

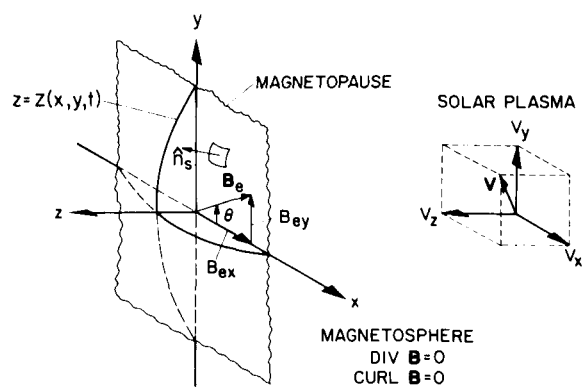

Figure 1.- View of coordinate system and an element of the magnetopause.

where the subscript e indicates values associated with the equilibrium configuration.

Solutions of the foregoing equations to be presented in the remainder of this paper are concerned with the behavior of limited portion of the magnetopause, and are expressed in terms of the local rectangular Cartesian coordinate system illustrated in figure 1. In all cases, the origin is placed at the center of the region of interest, either at or near the magnetopause, and the z axis is directed

normal to the boundary and into the magnetosphere. It is thus convenient to represent the coordinates of the boundary by $z = Z(x,y,t)$ where t represents time. Further, attention is confined to a sufficiently small portion of the magnetopause that Z is small compared not only with the over-all dimensions of the magnetosphere, such as the distance from the center of the earth to the nearest part of the magnetopause, say 60,000 km under representative conditions, but also with the dimensions in the x and y directions of the magnetopause element under consideration. The velocity of the undisturbed incident solar plasma is expressed in terms of the components V_x, V_y, V_z, and the unit vectors $\hat{i}$, $\hat{j}$, $\hat{k}$ parallel the x, y, z axes, respectively; thus,

$$\underset{\sim}{V} = \hat{i}V_x + \hat{j}V_y + \hat{k}V_z \tag{6}$$

The equilibrium magnetic field can be expressed similarly as

$$\underset{\sim}{B}_e = \hat{i}B_{e_x} + \hat{j}B_{e_y} + \hat{k}B_{e_z} \tag{7}$$

where $B_{e_x} = B_e \cos\theta$, $B_{e_y} = B_e \sin\theta$, and $B_{e_z} \approx 0$. The Cartesian components of the unit normal $\hat{n}_s$ to the magnetopause are

$$\hat{n}_s = \frac{\hat{i}(-\partial Z/\partial x) + \hat{j}(-\partial Z/\partial y) + \hat{k}}{[1 + (\partial Z/\partial x)^2 + (\partial Z/\partial y)^2]^{1/2}} \tag{8}$$

Since, furthermore,

$$\underset{\sim}{v} \cdot \hat{n}_s = (\partial Z/\partial t)\hat{k} \cdot \hat{n}_s \tag{9}$$

at any point xy on the magnetopause,

$$(\underset{\sim}{V} - \underset{\sim}{v}) \cdot \hat{n}_s = \frac{-V_x\partial Z/\partial x - V_y\partial Z/\partial y + V_Z - \partial Z/\partial t}{[1 + (\partial Z/\partial x)^2 + (\partial Z/\partial y)^2]^{1/2}} \tag{10}$$

The foregoing equations completely describe the mathematical model on which the remainder of the discussion is based. The remainder of this paper is concerned with the determination and discussion of solutions for the dynamical response of the magnetosphere boundary to a variety of initial displacements from equilibrium. It is assumed throughout that the undisturbed incident solar wind is uniform and steady in space and time.

FIRST-ORDER SOLUTION FOR SMALL AMPLITUDE WAVES ON AN OTHERWISE FLAT MAGNETOSPHERE BOUNDARY

Consider first the case of small amplitude waves of sufficiently short wavelength that curvature of the equilibrium magnetosphere boundary can be disregarded. Neglecting the effects of curvature is permissible under most

circumstances in which the wavelength is small compared with the radius of curvature of the equilibrium boundary. Under representative conditions, the latter dimension is of the order of 60,000 km or more everywhere except in a small region in the vicinity of each neutral point. It is further assumed that the ratio of the amplitude to the wavelength is sufficiently small that we can safely disregard all terms of higher order than the first in Z and its derivatives, where $z = 0$ is taken to represent the coordinates of the flat equilibrium boundary, and $z = Z(x,y,t)$ represents those of the perturbed boundary.

Under the above conditions, we can approximate $(\underset{\sim}{V} - \underset{\sim}{r}) \cdot \hat{n}_s$ by the numerator of the right side of equation (10), and its square by

$$[(\underset{\sim}{V} - \underset{\sim}{r}) \cdot \hat{n}_s]^2 = V_Z^2 \left[1 - 2\left(\frac{V_x}{V_Z}\frac{\partial Z}{\partial x} + \frac{V_y}{V_Z}\frac{\partial Z}{\partial y} + \frac{1}{V_Z}\frac{\partial Z}{\partial t}\right)\right] \tag{11}$$

The equilibrium magnetic field associated with the undisturbed flat boundary is simply $\underset{\sim}{B}_e = \text{const}$. The total field can be expressed by

$$\underset{\sim}{B} = \underset{\sim}{B}_e + \underset{\sim}{b} \tag{12}$$

where $\underset{\sim}{b}$ is a function of space and time that represents the perturbation magnetic field due to the departure of the magnetosphere boundary from its assumed flat equilibrium shape. To first order in $\underset{\sim}{b}$, we have

$$B^2 = \left[\left(B_{e_x} + b_x\right)^2 + \left(B_{e_y} + b_y\right)^2 + b_z^2\right]$$

$$\approx B_{e_x}^2 + B_{e_y}^2 + 2\left(B_{e_x}b_x + B_{e_y}b_y\right)$$

$$= B_e^2[1 + 2(b_x \cos\theta + b_y \sin\theta)/B_e] \tag{13}$$

Since the difference between the value for $\underset{\sim}{b}$ at the actual location of the boundary and at the equilibrium position ($z = 0$) is given by an expression of the form $(\partial\underset{\sim}{b}/\partial z)Z$ and is, hence, a product of small quantities, it is sufficient to evaluate B_s^2 at $z = 0$; thus,

$$B_s^2 = B_e^2[1 + 2(b_x \cos\theta + b_y \sin\theta)/B_e]_{z=0} \tag{14}$$

Substitution of equations (11) and (14) into equation (3) yields

$$\frac{B_e^2}{8\pi}\left[1 + 2\left(\frac{b_x \cos\theta + b_y \sin\theta}{B_e}\right)_{z=0}\right] = KmnV_z^2\left[1 - 2\left(\frac{V_x}{V_z}\frac{\partial Z}{\partial x} + \frac{V_y}{V_z}\frac{\partial Z}{\partial y} + \frac{1}{V_z}\frac{\partial Z}{\partial t}\right)\right] \tag{15}$$

Since the equilibrium surface lies in the xy plane, $\hat{n}_{se} = \hat{k}$ for this case, and equation (5) reduces to

$$B_e^2/8\pi = KmnV_z^2 \tag{16}$$

Combining equations (15) and (16) yields

$$\left(\frac{b_x \cos\theta + b_y \sin\theta}{B_e}\right)_{z=0} = -\left(\frac{V_x}{V_z}\frac{\partial Z}{\partial x} + \frac{V_y}{V_z}\frac{\partial Z}{\partial y} + \frac{1}{V_z}\frac{\partial Z}{\partial t}\right) \tag{17}$$

The right side of equation (17) can be simplified by transforming to a coordinate system fixed with respect to the tangential component of the solar wind. We thus introduce the new variables

$$\xi = x - V_x t\ , \qquad \eta = y - V_y t\ , \qquad \zeta = z\ , \qquad \tau = t \tag{18}$$

Equation (17) thus becomes

$$\left(\frac{b_\xi \cos\theta + b_\eta \sin\theta}{B_e}\right)_{\zeta=0} = -\frac{1}{V_z}\frac{\partial Z}{\partial \tau} \tag{19}$$

In order to proceed further, it is necessary to determine the appropriate relation between $\underset{\sim}{b}$ and Z. Substitution of equation (12) into equation (1), with $\underset{\sim}{B}_e$ = const, shows that div $\underset{\sim}{b}$ = 0 and curl $\underset{\sim}{b}$ = 0. This implies that

$$\underset{\sim}{b} = -\text{grad}\ \Omega \tag{20}$$

where Ω is a solution of Laplace's equation

$$\nabla^2 \Omega = 0 \tag{21}$$

The boundary conditions for $\underset{\sim}{b}$ are that

$$(\underset{\sim}{b})_{\zeta=\infty} = 0 \tag{22}$$

and

$$\left(\frac{b_\zeta}{B_e}\right)_{\zeta=0} = \frac{dZ}{ds} = \frac{\partial Z}{\partial \xi}\frac{d\xi}{ds} + \frac{\partial Z}{\partial \eta}\frac{d\eta}{ds} = \frac{\partial Z}{\partial \xi}\cos\theta + \frac{\partial Z}{\partial \eta}\sin\theta \tag{23}$$

The corresponding conditions for Ω are

$$(\Omega)_{\zeta=\infty} = \text{const} \tag{24}$$

which can be equated to zero without loss of generality, and

$$-\frac{1}{B_e}\left(\frac{\partial \Omega}{\partial \zeta}\right)_{\zeta=0} = \frac{\partial Z}{\partial \xi}\cos\theta + \frac{\partial Z}{\partial \eta}\sin\theta \tag{25}$$

A general solution of equation (21) that vanishes at infinite ζ can be found by separation of variables to be a summation of terms of the form

$$\Omega = (A \sin k_1\xi + B \cos k_1\xi)(C \sin k_2\eta + D \cos k_2\eta)\exp[-(k_1^2 + k_2^2)^{1/2}\zeta] \tag{26}$$

in which the integration constants may vary with time. If attention is confined to wavelike boundary perturbations having nodal lines at $\tau = 0$ arranged in the form of a rectangular grid, and the coordinate system is oriented without further restriction so that the ξ and η axes are parallel the nodal lines at that time, we can write

$$(Z)_{\tau=0} = \epsilon(0) \cos k_1\xi \cos k_2\eta \tag{27}$$

The proper evaluation of the coefficients of equation (26) so as to satisfy equations (25) and (27) yields the following expression for Ω at $\tau = 0$:

$$(\Omega)_{\tau=0} = -\epsilon(0)\left(\frac{k_1}{k}\cos\theta\,\sin k_1\xi\,\cos k_2\eta + \frac{k_2}{k}\sin\theta\,\cos k_1\xi\,\sin k_2\eta\right)e^{-k\zeta} \tag{28}$$

where

$$k = (k_1^2 + k_2^2)^{1/2} \tag{29}$$

The left side of equation (19) thus becomes, at $\tau = 0$

$$\left(\frac{b_\xi\cos\theta + b_\eta\sin\theta}{B_e}\right)_{\substack{\zeta=0\\ \tau=0}} = \frac{\epsilon(0)}{k}[(k_1^2\cos^2\theta + k_2^2\sin^2\theta)\cos k_1\xi\,\cos k_2\eta$$

$$- 2k_1k_2\sin\theta\cos\theta\sin k_1\xi\,\sin k_2\eta] \tag{30}$$

It is convenient to restrict attention at this point to the not inconsiderable class of cases in which any one of the following additional conditions hold

$$\sin\theta = 0\,, \quad \cos\theta = 0\,, \quad k_1 = 0\,, \quad k_2 = 0 \tag{31}$$

The first two conditions permit the wavelength to be arbitrary in both directions but require that the equilibrium magnetic field be parallel to either of the two sets of nodal lines of the initial boundary perturbations. The latter two conditions permit arbitrary orientation of the nodal lines and the equilibrium magnetic field, but require that the boundary perturbation be two-dimensional, that is, have the form of cylindrical corrugations. Equations (19) and (30) indicate that the nodal lines remain fixed for all time for these cases, and that the solution is given by

$$Z = \epsilon(\tau)\cos k_1\xi\,\cos k_2\eta \tag{32}$$

where the amplitude $\epsilon(\tau)$ satisfies the equation

$$\frac{d\epsilon}{d\tau} = \frac{-V_Z(k_1^2\cos^2\theta + k_2^2\sin^2\theta)\epsilon}{k} = -K_o\epsilon \tag{33}$$

The solution is

$$\epsilon = \epsilon_o e^{-K_o\tau} \tag{34}$$

where ϵ_o represents the amplitude at $\tau = 0$; that is, $\epsilon_o = \epsilon(0)$. It should be observed that the behavior of the boundary is considerably more complicated if none of the four conditions given in equations (31) apply, since then $(\partial Z/\partial \tau)_{\tau=0}$ fails to vanish on the nodal lines where $(Z)_{\tau=0} = 0$ and the form of the boundary perturbation depart immediately from the original $\cos k_1\xi \cos k_2\eta$ form.

Substitution into equations (32), (33), and (34) of the original physical variables using the relations given by equation (19) yields

$$Z = \epsilon_o e^{-t/t_o^*}[\cos k_1(x - V_x t)][\cos k_2(y - V_y t)] \tag{35}$$

where the time constant t_o^* is given by

$$t_o^* = \frac{1}{K_o} = \frac{k}{V_z(k_1^2 \cos^2\theta + k_2^2 \sin^2\theta)}$$

$$= \frac{(\lambda_x^2 + \lambda_y^2)^{1/2}}{2\pi V_z}\left(\frac{\lambda_x\lambda_y}{\lambda_x^2 \sin^2\theta + \lambda_y^2 \cos^2\theta}\right) \tag{36}$$

and

$$\lambda_x = 2\pi/k_1 , \qquad \lambda_y = 2\pi/k_2 \tag{37}$$

represent the wavelengths measured in the x and y directions, respectively. Two general conclusions follow immediately from the above results. The first is that the presence of the quantities $x - V_x t$ and $y - V_y t$ in the arguments of the cosines of equation (35) indicates that the wave system drifts along the magnetosphere boundary with the tangential component of the solar wind. The second is that the time constant t_o^* is positive, indicating that the waves damp with time, or at least never grow.

If k_1 or k_2 vanishes, the boundary perturbations are two-dimensional corrugations with the nodal lines and other generators parallel to the x or y axis, respectively. The time constants for these cases are given by

$$(t_o^*)_{\lambda_x=\infty} = \frac{\lambda_y}{2\pi V_z \sin^2\theta} , \qquad (t_o^*)_{\lambda_y=\infty} = \frac{\lambda_x}{2\pi V_z \cos^2\theta} \tag{38}$$

A plot of the variation of $(t_o^*)_{\lambda_y=\infty}$ with wavelength λ_x for various orientations θ of the equilibrium magnetic field is shown in figure 2 for a representative case in which $V_z = 500$ km/sec. We see, for instance, that the time constant for decay of corrugations having east-west generators ($\lambda_y = \infty$) and situated near the equatorial plane ($\theta = 0^\circ$) is of the order of a second for wavelengths as great as 3000 km, and proportionally less for shorter wavelengths. It increases to infinity, implying no damping, as θ goes to 90° and the nodal lines are rotated so as to become parallel to the geomagnetic field lines. This example illustrates the general result that corrugations having generators alined with the equilibrium field are neutrally stable to first order in small perturbations. This case will, therefore, be re-examined to higher order of accuracy subsequently herein.

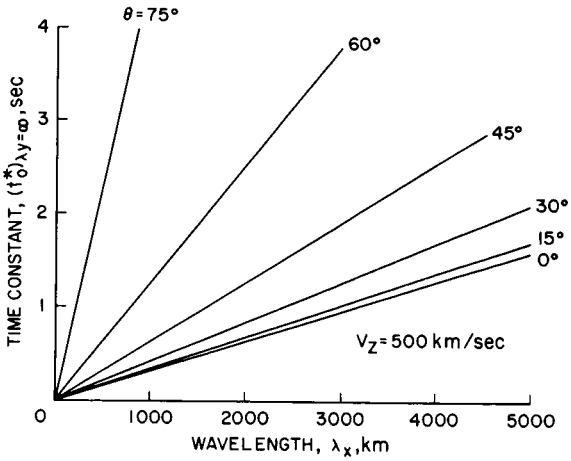

Figure 2.- Variation of time constant with wavelength for two-dimensional corrugations on a flat equilibrium boundary.

If, on the other hand, neither k_1 nor k_2 vanishes, but $\theta = 0^\circ$ or 90°, so that the nodal lines form a rectangular grid and the equilibrium field lines are alined with one set of nodal lines, we have the following expressions for the time constant

$$(t_o^*)_{\theta=0} = \frac{(\lambda_x^2 + \lambda_y^2)^{1/2}}{2\pi V_z}\left(\frac{\lambda_x}{\lambda_y}\right), \qquad (t_o^*)_{\theta=\pi/2} = \frac{(\lambda_x^2 + \lambda_y^2)^{1/2}}{2\pi V_z}\left(\frac{\lambda_y}{\lambda_x}\right) \qquad (39)$$

This result shows the time constant is inversely proportional to V_z, linearly proportional to the mean scale of the wave system $(\lambda_x^2 + \lambda_y^2)^{1/2}$, and depends, in addition, on the ratio of wavelengths in the x and y directions. A plot of the results for $(t_o^*)_{\theta=\pi/2}$ for $V_z = 500$ km/sec is shown in figure 3. We see, once again, that the time constant is of the order of a second for a wide variety of conditions when mean wavelengths of the order of a few thousand kilometers are considered. It should be noted that figure 3 is not appropriate for displaying the time constants for a two-dimensional corrugation since then $(\lambda_x^2 + \lambda_y^2)^{1/2}$ goes to infinity and an indeterminate form appears. Results for this case are given correctly by equation (39), however, or, more

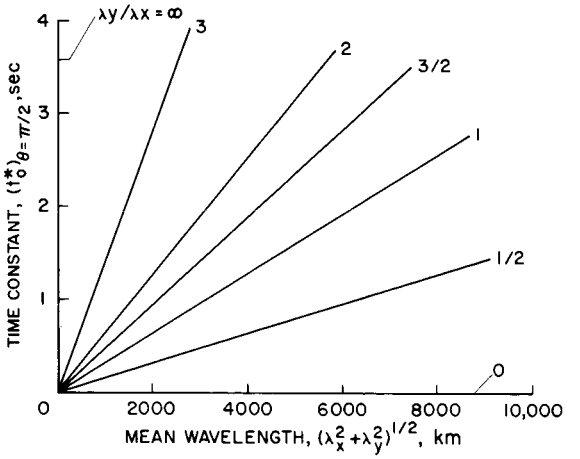

Figure 3.- Variation of time constant with mean wavelength for rectangular wave grid on a flat equilibrium boundary.

explicitly and more generally with respect to the relative orientation of the directions of the nodal lines and the equilibrium field, by equations (38).

From the above, we conclude that long wavelength waves die out slower than short wavelength waves, that rectangular grid distortions die out slower when the wavelength is longer in the direction of the field than in the direction normal to the field, and that two-dimensional distortions having nodal lines alined with the equilibrium field direction do not damp at all, when only first-order terms are retained in the analysis. It follows in addition, that, if the boundary is initially disturbed in such a way that it can be represented by an arbitrary distribution of waves having the forms described above, all components would damp with the passage of time, except those that are two-dimensional and have their nodal lines alined with the equilibrium field direction. These alone would remain, and they would drift along the boundary with a speed equal to the tangential component of the solar wind, neither damping nor amplifying as they travel. Since this component vanishes at the nose of the magnetosphere near the subsolar point and increases to the full speed $V = (V_x^2 + V_y^2 + V_z^2)^{1/2}$ of the undisturbed incident stream far downstream of the earth, the waves tend to drift very slowly near the magnetosphere nose, but accelerate to several hundred kilometers per second along the flanks. The results for all the waves considered show, moreover, that the time constant is inversely proportional to the normal component V_z of the solar wind velocity. Since V_z equals V at the magnetosphere nose, and decreases to zero along the flanks, the time constant grows indefinitely with distance along the magnetosphere boundary from the nose, indicating that boundary perturbations damp much more slowly on the flanks of the magnetosphere than on the nose. We thus find that all except alined waves tend to damp rapidly with very little drift near the nose of the magnetosphere, but damp slowly as they run rapidly along the flanks.

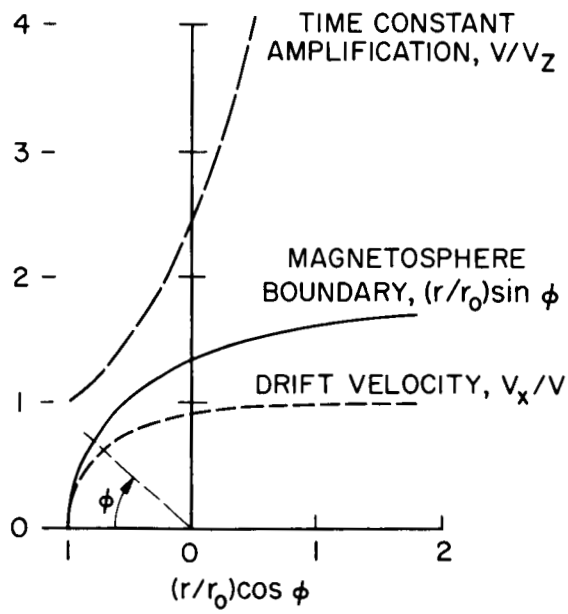

Figure 4.- Variation of lateral coordinate of magnetosphere boundary, $(r/r_0)\sin\varphi$, time constant amplification (V/V_z), and drift velocity (V_x/V) with geocentric distance along a line parallel the solar wind direction.

Figure 4 has been included to give a more quantitative understanding of the degree to which the time constant and drift velocity change along the equatorial portion of the magnetosphere boundary. The solid curve shows the equatorial trace of the magnetosphere boundary calculated under the usual assumption that the geomagnetic field in the equatorial plane varies as the inverse cube of the distance from the center of the earth (Ferraro, ref. 18; Beard, ref. 19; Spreiter and Briggs, ref. 14; etc.), and normalized by dividing by the geocentric distance r_0 to the magnetosphere nose. The dashed curves show the time constant amplification factor V/V_z and the

normalized drift velocity V_x/V as a function of $(r/r_o)\cos\varphi$ where r represents the geocentric distance to the boundary and φ is a longitude angle measured from the direction of approach of the undisturbed incident solar wind. They are calculated using the relations

$$V/V_z = (r/r_o)^3 \tag{40}$$

$$V_x/V = [1 - (r_o/r)^6]^{1/2} \tag{41}$$

FIRST-ORDER SOLUTION FOR SMALL AMPLITUDE WAVES ON A SLIGHTLY CURVED MAGNETOSPHERE BOUNDARY

The preceding analysis will now be extended to include the effect of slight curvature of the equilibrium magnetosphere boundary. We again neglect all terms of higher order than the first in $\bar{Z}$, where $\bar{Z}(x,y,t) = Z - Z_e$ represents the displacement Z of the perturbed magnetopause relative to the displacement Z_e of the curved equilibrium surface and confine attention to the case in which the radius of curvature of the equilibrium surface is much greater than both the wavelength and amplitude of the boundary perturbations. Under these circumstances, it is permissible to represent the effects of boundary displacement from $z = 0$ at any point by superposition of effects of the equilibrium curvature displacement and the perturbation displacement. The equilibrium magnetic field can no longer be regarded as a constant in a region extending several wavelengths in all directions inside the magnetosphere from the origin, as indicated previously in connection with equation (12), however, since the irrotationality condition given by equation (1) indicates a nonvanishing field gradient at a curved boundary. The consequences of this condition can be illustrated in terms of a local coordinate system in which the σ axis is alined with the equilibrium magnetic field vector and the ν axis is the normal to the σ axis in the plane determined by the local curvature of the field line. Then curl $\underset{\sim}{B} = 0$ evaluated at the equilibrium surface leads to

$$\left(\frac{\partial B_\sigma}{\partial \nu}\right)_s = \left(\frac{\partial B_\nu}{\partial \sigma}\right)_s \approx \frac{B_{se}}{R} \tag{42}$$

where B_{se} refers to the magnitude of $\underset{\sim}{B}_e$ at the equilibrium surface, and R refers to the local radius of curvature of the field line. Since ν is thus very nearly parallel to the direction of z for the conditions described, we have the following expression for the equilibrium magnetic field $\underset{\sim}{B}_e$ in the vicinity of the magnetopause

$$\underset{\sim}{B}_e = \underset{\sim}{B}_{se}\left(1 + \frac{z - Z_e}{R}\right) = \underset{\sim}{B}_{se}\left(1 + \frac{\bar{z}}{R}\right) \tag{43}$$

The total field at the boundary is thus

$$\underset{\sim}{B}_s = \underset{\sim}{B}_{se}\left(1 + \frac{\overline{Z}}{R}\right) + \underset{\sim}{b}_s \tag{44}$$

where $\underset{\sim}{b}_s$ is the perturbation field associated with the departures $\overline{Z}$ from the equilibrium surface. The perturbation field may be evaluated in the same way as in the preceding section for the flat equilibrium boundary. The result for a perturbation shape defined by $\overline{Z}(x,y)$ is found to be the same as determined before for a perturbation shape defined by $Z(x,y)$. The counterpart of equation (15) is thus

$$\frac{B_{se}^2}{8\pi}\left[1 + \frac{2\overline{Z}}{R} + 2\left(\frac{b_x \cos\theta + b_y \sin\theta}{B_{se}}\right)_{\overline{Z}=0}\right] = KmnV_z^2\left[1 - 2\left(\frac{V_x}{V_z}\frac{\partial Z}{\partial x} + \frac{V_y}{V_z}\frac{\partial Z}{\partial y} + \frac{1}{V_z}\frac{\partial Z}{\partial t}\right)\right] \tag{45}$$

Subtracting the corresponding expression for the equilibrium state

$$\frac{B_{se}^2}{8\pi} = KmnV_z^2\left[1 - 2\left(\frac{V_x}{V_z}\frac{\partial Z_e}{\partial x} + \frac{V_y}{V_z}\frac{\partial Z_e}{\partial y}\right)\right] \tag{46}$$

and retaining only terms of first order in b_x, b_y, and $\overline{Z}$ yields

$$\frac{\overline{Z}}{R} + \left(\frac{b_x \cos\theta + b_y \sin\theta}{\overline{B}_{se}}\right)_{\overline{Z}=0} = -\left(\frac{V_x}{V_z}\frac{\partial \overline{Z}}{\partial x} + \frac{V_y}{V_z}\frac{\partial \overline{Z}}{\partial y} + \frac{1}{V_z}\frac{\partial \overline{Z}}{\partial t}\right) \tag{47}$$

where $\overline{B}_{se}$ is a constant equal to the value of B_{se} at, say, the origin.

Introducing the variables ξ, η, ζ, τ, defined by equations (18) transforms equation (47) into

$$\frac{\overline{Z}}{R} + \left(\frac{b_\xi \cos\theta + b_\eta \sin\theta}{\overline{B}_{se}}\right)_{\overline{Z}=0} = -\frac{1}{V_z}\frac{\partial \overline{Z}}{\partial \tau} \tag{48}$$

If attention is restricted to the class of cases for which any one of the four conditions given by equations (31) holds, the same line of reasoning as that described previously to solve equation (19) shows that the solution is given by

$$\bar{Z} = \epsilon(\tau)\cos k_1\xi \cos k_2\eta \tag{49}$$

where $\epsilon(\tau)$ is given by

$$\epsilon = \epsilon_o e^{-\tau/t^*} \tag{50}$$

ϵ_o represents the amplitude at $\tau = 0$, and

$$t^* = \left[V_z\left(\frac{1}{R} + \frac{k_1^2\cos^2\theta + k_2^2\sin^2\theta}{k}\right)\right]^{-1}$$

$$= \left\{V_z\left[\frac{1}{R} + \frac{2\pi(\lambda_y^2\cos^2\theta + \lambda_x^2\sin^2\theta)}{\lambda_x\lambda_y(\lambda_x^2 + \lambda_y^2)^{1/2}}\right]\right\}^{-1} = \left(\frac{V_z}{R} + \frac{1}{t_o^*}\right)^{-1} = \frac{t_o^*}{1 + V_z t_o^*/R} \tag{51}$$

where λ_x and λ_y represent the wavelengths in the x and y directions as defined by equation (37), and t_o^* is the time constant defined by equation (36). In terms of the original variables, equations (49) and (50) are

$$\bar{Z} = \epsilon_o e^{-t/t^*}[\cos k_1(x - V_x t)][\cos k_2(y - V_y t)] \tag{52}$$

This result shows, again, that the wave system drifts along the magnetosphere boundary with the tangential component of the solar wind, and that the amplitude damps with a time constant t^*. Now, for $R = \infty$, t^* is always positive, and the wave amplitude can never grow, as discussed in the preceding section. When R is finite, however, more possibilities arise. If R is positive (the center of curvature of the equilibrium surface is on the magnetic field side of the boundary, that is, inside the magnetosphere), $t^* < t_o^*$ and the effect of curvature is to reduce the time constant or, equivalently, to increase the rate at which the disturbed boundary returns toward the equilibrium shape. If, on the other hand, R is negative, the possibility exists that t^* may become negative, indicating that boundary perturbations grow in amplitude with time. The critical radius R_{cr} for neutral stability is obtained by equating t^* to infinity and solving. The result is

$$R_{cr} = -V_z t_o^* = -\left[\frac{\lambda_x\lambda_y(\lambda_x^2 + \lambda_y^2)^{1/2}}{2\pi(\lambda_x^2\sin^2\theta + \lambda_y^2\cos^2\theta)}\right] \tag{53}$$

If the nodal lines of the perturbation wave system form a square grid, that is, $\lambda_x = \lambda_y = \lambda$, equation (53) reduces to

$$R_{cr} = -\sqrt{2}\lambda/2\pi \tag{54}$$

The formal analysis thus indicates that the boundary is unstable to small disturbances if the center of curvature is outside the magnetosphere and the radius of curvature of the equilibrium surface is less than $\sqrt{2}\pi$ times the perturbation wavelength. Since the latter is required to be much less than the radius of curvature at the outset of this analysis, it must be concluded that all square grid boundary perturbations for which the present results are applicable are stable in spite of possible destabilizing influences due to curvature of the equilibrium surface.

If k_1 or k_2 vanishes and the boundary perturbations are two-dimensional corrugations as noted previously, the time constants are given by

$$(t^*)_{\lambda_x=\infty} = \left[V_z \left(\frac{1}{R} + \frac{2\pi \sin^2 \theta}{\lambda_y} \right) \right]^{-1} \tag{55}$$

$$(t^*)_{\lambda_y=\infty} = \left[V_z \left(\frac{1}{R} + \frac{2\pi \cos^2 \theta}{\lambda_x} \right) \right]^{-1} \tag{56}$$

Since λ_x and λ_y are supposed to be very much smaller than $|R|$ in the present analysis, we see that instability (negative t^*) occurs only for very small θ if $\lambda_x = \infty$, or for θ very nearly equal to $\pi/2$ if $\lambda_y = \infty$. For example, if $\lambda_x = \infty$, $\lambda_y = 1000$ km, and $R = -60{,}000$ km, $|\sin\theta| = (120\pi)^{-1/2} = 0.0515$. The critical values for θ are thus about $\pm 3^\circ$ for two-dimensional boundary perturbations having nodal lines alined with the x axis. We can conclude alternatively by a simple rotation of the coordinate system that only those waves having their nodal lines within 3° of the direction of the field lines will grow with time. All others will damp out, and eventually disappear. For other values for λ_y and R, the numerical results will, of course, differ. Figure 5 is a plot of the variation with θ of the critical value of the ratio λ_y/R for waves having $\lambda_x = \infty$. Two-dimensional corrugations having λ_y/R less than that indicated by the curve

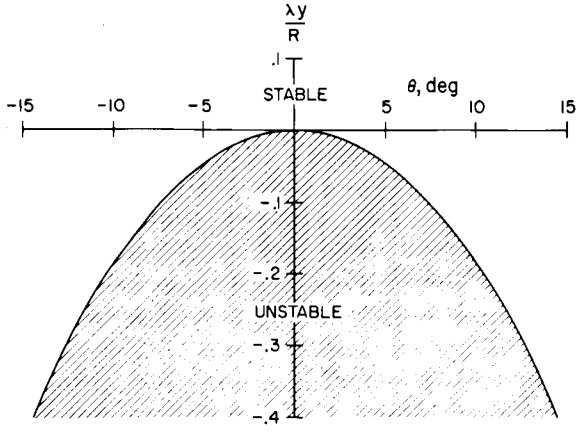

Figure 5.- Stability boundary for two-dimensional corrugations ($\lambda_x = \infty$) on a curved equilibrium surface.

are unstable and, conversely, as indicated. Thus, on a flat surface for which $R = \infty$ and $\lambda_y/R = 0$, all two-dimensional waves are stable, except those perfectly alined with the field direction ($\theta = 0^o$) which have neutral stability. All waves on equilibrium surfaces with $R > 0$ are also stable, but those sufficiently closely alined with the field are unstable on equilibrium surfaces with $R < 0$. Although $R > 0$ nearly everywhere on the magnetosphere boundary, both cases occur. In particular, negative values for R occur in limited regions in the immediate vicinity of the neutral points N, as illustrated in figure 6 by the dotted portions of traces of the magnetosphere boundary (ref. 19). Also included and indicated by dashed lines are several magnetic field lines for the noon-midnight meridian plane, as given by Mead (ref. 20).

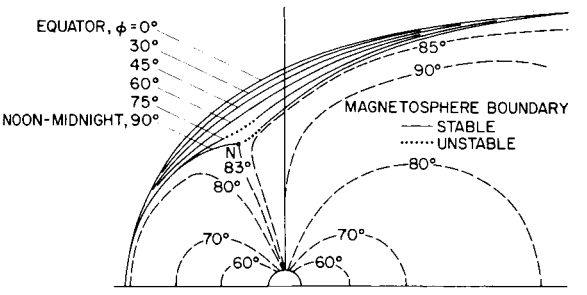

Figure 6.- Traces of the magnetosphere boundary in the equatorial plane, noon-midnight meridian plane, and several intermediate planes (ref. 19). Magnetic field lines in the noon-midnight meridian plane (ref. 20).

Since only the nearly alined two-dimensional waves are significantly affected by curvature of the equilibrium surface, it is of interest to examine the special form to which equations (55) and (56) simplify for perfectly alined waves, namely

$$t^* = R/V_z \tag{57}$$

The time constant is thus equal to the time required for a particle with velocity V_z to travel a distance R. Representative values for conditions at the nose of the magnetosphere may be $R = 60{,}000$ km and $V_z = 500$ km/sec, for which $t^* = 120$ sec. The time constant increases beyond all bounds at the neutral points and also far downstream along the flanks of the magnetosphere boundary, since V_z approaches zero and R does not vanish. Alined two-dimensional boundary perturbations thus neither damp nor grow as they drift along the magnetosphere boundary in these regions. A short distance downstream from the neutral point, we may have $R = -60{,}000$ km and $V_z = 100$ km/sec, in which case $t^* = -60$ sec, and the waves grow with time. In all cases, the time constant is long compared with the values representative of less elongated rectangular grid perturbations.

The small regions of instability near the neutral points are of particular interest because they provide a means by which solar plasma can be constantly admitted into the magnetosphere, and may very well be associated with the constant magnetic agitation of the polar regions, as summarized, for instance, by Fukushima (ref. 21). He assembled a considerable body of ground-based magnetometer data gathered during the IGY (July 1957 - December 1958) and the Second Polar Year (August 1932 - August 1933), and analyzed it in various ways according to the time of day and year, and the degree of disturbance of the world-wide geomagnetic field. The results show that the polar regions are constantly disturbed, even at periods when the planetary geomagnetic field is very quiet. Two of the many summary plots presented by Fukushima are

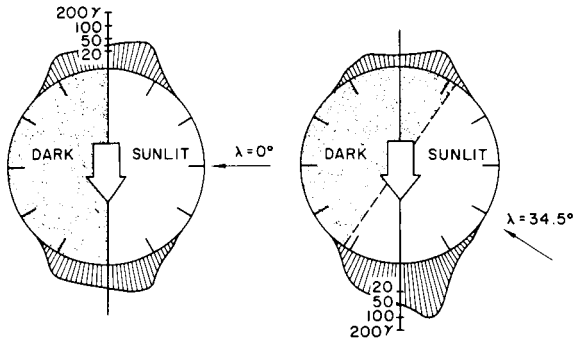

Figure 7.- Polar magnetic disturbance near the noon and midnight meridians at times during the IGY when $K_p = 0_o$ and the sun-earth line is inclined at 0^o and 34.5^o to the geomagnetic equatorial plane (ref. 21).

reproduced in figure 7. These show the latitudinal distribution of the average geomagnetic disturbance near the noon and midnight meridians for the case of $K_p = 0_o$, that is, for the very quietest times as indicated by the planetary geomagnetic index, at two selected sets of times extending over the entire period of the IGY. The results show that the magnitude of the polar-cap disturbance is of the order of a few or several tens of gammas, that both polar caps are equally disturbed when the sun-earth line is perpendicular to the geomagnetic dipole axis, and that the disturbances are a maximum at summer noon, and a minimum at winter midnight. These results, when taken in conjunction with the corresponding changes in the locations of the neutral points, such as calculated by Spreiter and Briggs (ref. 14), appear consistent with what might be anticipated on the basis of direct invasion of charged particles or propagation of hydromagnetic waves into the polar regions along the field lines from the vicinity of the neutral points on the magnetosphere boundary.

EXACT SOLUTION FOR ALINED WAVES ON A FLAT MAGNETOSPHERE BOUNDARY

The anlysis presented in the preceding sections is restricted to consideration of only first-order terms in the perturbation quantities. It is thus sufficient for the analysis of decaying waves of small amplitude, and of the initial behavior of amplifying waves. It cannot be used, however, to provide information on the subsequent behavior of amplifying waves. Although the general treatment of such cases presents a very complex problem, the analysis of the special case of alined two-dimensional waves on a flat equilibrium surface, while nonlinear, remains tractable. This case is, moreover, an informative one since such waves were found in the first-order analysis to be neutrally stable, and a more accurate analysis is required to elucidate their properties.

For sake of definiteness, consider the equilibrium magnetic field to be in the direction of the positive y axis, and that the distortions of the boundary surface change with x, but not with y. For such two-dimensional, or cylindrical, alined boundary distortions, the perturbation magnetic field vanishes and the total field remains constant and equal to the value B_e for the flat equilibrium surface. Equation (3) thus becomes

$$\frac{B_e^2}{8\pi} = Kmn \left[\frac{(-V_x \, \partial Z/\partial x + V_z - \partial Z/\partial t)^2}{1 + (\partial Z/\partial x)^2} \right] \tag{58}$$

and when combined with the corresponding equilibrium relation given by equation (16) yields

$$\left(1 - \frac{V_x^2}{V_z^2}\right)\left(\frac{\partial Z}{\partial x}\right)^2 - \frac{1}{V_z^2}\left(\frac{\partial Z}{\partial t}\right)^2 + \frac{2V_x}{V_z}\frac{\partial Z}{\partial x} - \frac{2V_x}{V_z^2}\frac{\partial Z}{\partial x}\frac{\partial Z}{\partial t} + \frac{2}{V_z}\frac{\partial Z}{\partial t} = 0 \qquad (59)$$

Introducing the new variables

$$\xi = x - V_x t\ , \qquad \tau = V_z t\ , \qquad \bar{Z} = Z - \tau \qquad (60)$$

yields

$$\left(\frac{\partial \bar{Z}}{\partial \xi}\right)^2 - \left(\frac{\partial \bar{Z}}{\partial \tau}\right)^2 + 1 = 0 \qquad (61)$$

It can be demonstrated by differentiation that a solution of equation (61) is

$$(\bar{Z} - A)^2 + (\xi - B)^2 = (\tau - C)^2 \qquad (62)$$

The equivalent expression in terms of the original variables is

$$(Z - V_z t - A)^2 + (x - V_x t - B)^2 = (V_z t - C)^2 \qquad (63)$$

This solution represents a circle with center at $z_c = V_z t + A$, $x_c = V_x t + B$, and radius $|V_z t - C|$. We can set $B = 0$ without loss of generality by locating the coordinate system so that the center of the circle is on the $\xi = x - V_x t = 0$ axis and, hence, drifts with the tangential component of the solar wind. The remaining integration constants A and C can be evaluated by letting $t = T$ at the instant when the center of the circle is at the origin, and noting that $z = Z_m = \pm\epsilon_o$ at $\xi = 0$ for all time. The latter condition follows from the fact that $\partial Z/\partial \xi = 0$ at $\xi = 0$ for the choice of coordinate system described above, together with the consequence indicated by equation (59) that $\partial Z/\partial t = 0$ at such a point. In this way equation (63) becomes

$$[Z - V_z(t - T)]^2 + (x - V_x t)^2 = [V_z(t - T) - Z_m]^2 \qquad (64)$$

The boundary perturbation is thus described by a circular arc of radius R given by

$$R = |V_z(t - T) - Z_m| \tag{65}$$

with its center located at

$$x_c = V_x t , \qquad z_c = V_z(t - T) \tag{66}$$

The center thus moves with the velocity components of the undisturbed incident solar wind V_x and V_z. Although this solution is not useful for determining the dynamical response of the magnetosphere boundary to an initial disturbance in the form of a periodic wave, it is appropriate for the study of the response of the boundary to an initial displacement in the form of a solitary segment of a circle. This is not too restricting to render the solution uninteresting, however, since the region of maximum displacement of any continuous distortion will approximate a circle in form.

Two cases are possible, depending on whether the circular segment bulges in the direction of the plasma or the field side of the boundary, or equivalently on whether Z_m is negative or positive. The case of negative Z_m illustrated in figure 8 will be considered first. An expression for the half width W at $t > T$ for this case can be obtained readily from equation (63) by equating x to W, Z to 0, and solving for W. It is

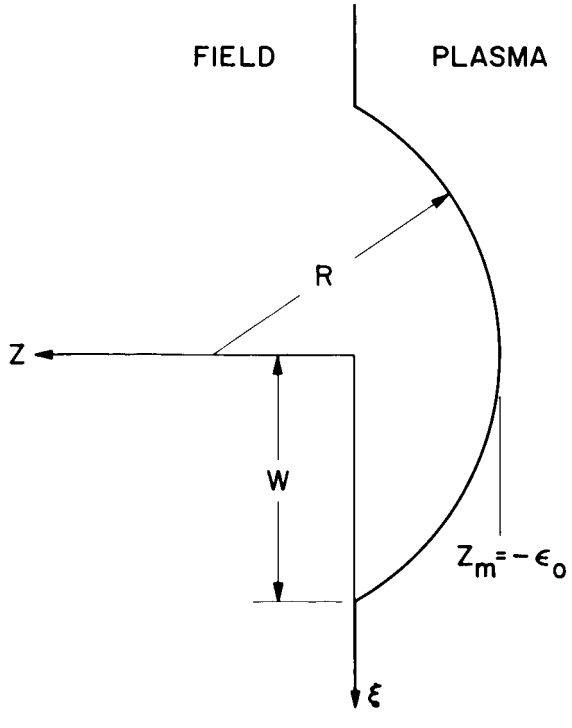

Figure 8.- View of trace in ξ,z plane of perturbed boundary with negative Z_m.

$$W = V_z(t - T)\left\{\left[1 + \frac{\epsilon_o}{V_z(t - T)}\right]^2 - 1\right\}^{1/2} \tag{67}$$

At great time, that is when $\epsilon_o/V_z(t - T) \ll 1$, W grows with time approximately as

$$W \approx [2V_z\epsilon_o(t - T)]^{1/2} \tag{68}$$

With V_z = 500 km/sec = 5×10^7 cm/sec, ϵ_o = 100 km = 10^7 cm, and an initial half width W_i = 1000 km = 10^8 cm which according to equation (68) occurs at $t_i - T$ = 10 sec, W in cm is

$$W = \left(\frac{t - T}{t_i - T}\right)^{1/2} \times 10^8 = \left(1 + \frac{t - t_i}{10}\right)^{1/2} \times 10^8 \text{ cm} \qquad (69)$$

It thus requires 30 sec to double the width of the bulge, and 150 sec to quadruple the width. Since the maximum displacement $|Z_m|$ remains constant as the width increases, the bulge clearly smooths out with the passage of time. It should be observed, however, that this process is slow compared with the rates charcteristic of unalined waves.

We next consider the alternative case of a dent into the magnetic field side of the boundary. Such a boundary perturbation is characterized by a positive value for $Z_m = \epsilon_o$ and negative $t - T$, as illustrated in figure 9. The half width W of such a dent is given for $t < T$ by

$$W = V_z(T - t)\left\{\left[1 + \frac{\epsilon_o}{V_z(T - t)}\right]^2 - 1\right\}^{1/2} \qquad (70)$$

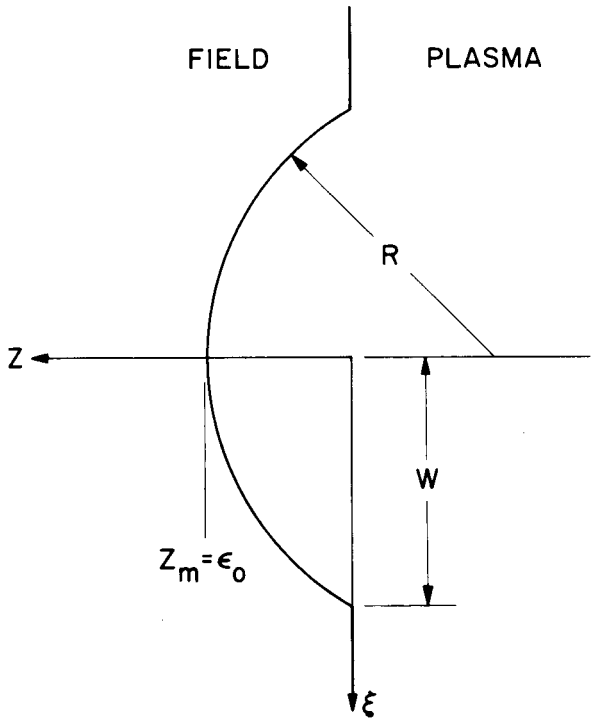

Figure 9.- View of trace in ξ,z plane of perturbed boundary with positive Z_m.

At great values for $T - t$, this expression approximates

$$W \approx [2V_z\epsilon_o(T - t)]^{1/2}$$

$$= \{2V_z\epsilon_o[(T - t_i) - (t - t_i)]\}^{1/2} \qquad (71)$$

Thus, with increasing t, W diminishes with a rate dW/dt that increases with time. If, for example, at an initial instant $t = t_i$, $W = 1000$ km, $V_z = 500$ km/sec, $\epsilon_o = 100$ km, equation (71) indicates that $T - t_i = 10$ sec. At a time 5 sec after t_i, $W = 707$ km, and 5 sec later still equation (71) indicates that $W = 0$. Equation (71) is not sufficiently accurate for the latter time, however, and the more complete relation given by equation (70) shows, in fact, that $W = \epsilon_o$. The initially shallow dent thus collapses to a semicircle in 10 sec. This configuration marks an obvious limit of which the above analysis may be employed to determine the shape of the entire dent. As indicated by equations (64) through (66), the center of the circle describing the dent moves to positive z at subsequent times. If this solution were

used to describe the shape of the entire dent, part of the surface would be shielded from the solar wind, and the condition specified by equation (4) would not be satisfied.

The appropriate solution for the model defined by equations (1) through (5) is as follows for the further development of the dent following the time $t = T$ at which the dent is semicircular with the center of the origin. The portion of the dent that penetrates most deeply into the magnetosphere is semicircular and defined for $z > z_c$ by equation (64). The remainder of the boundary connecting the ends of the semicircle and the undeformed equilibrium portion of the boundary is straight and parallel to the z axis. This follows from the fact that the magnetic pressure on this portion of the boundary, as indeed on the entire boundary in this example, is equal to $B_s^2/8\pi = KmnV_z^2$. Since $\hat{n}_s = \pm\hat{i}$ on these segments of the boundary, equation (3) shows that

$$KmnV_z^2 = Kmn(V_x - v_x)^2 \tag{72}$$

Hence,

$$|v_x - V_x| = V_z \tag{73}$$

where v_x represents the velocity of the boundary, positive in the direction of the positive x axis, and the signs are associated with the two segments in such a way that the straight-sided intrusion into the magnetosphere collapses rather than expands with the passage of time. Viewed in the ξ,z coordinate system that drifts along the boundary with the tangential component of the solar wind V_x, the straight segments travel toward the z axis with a uniform velocity equal to V_z. The straight sides thus remain connected to the ends of the semicircle, and all conditions are satisfied. The resulting form of the indentation is illustrated in figure 10 for the set of numerical conditions given above following equation (71). Of particular note is the result that the dent collapses from a semicircle to a line along the z axis in 1/5 sec.

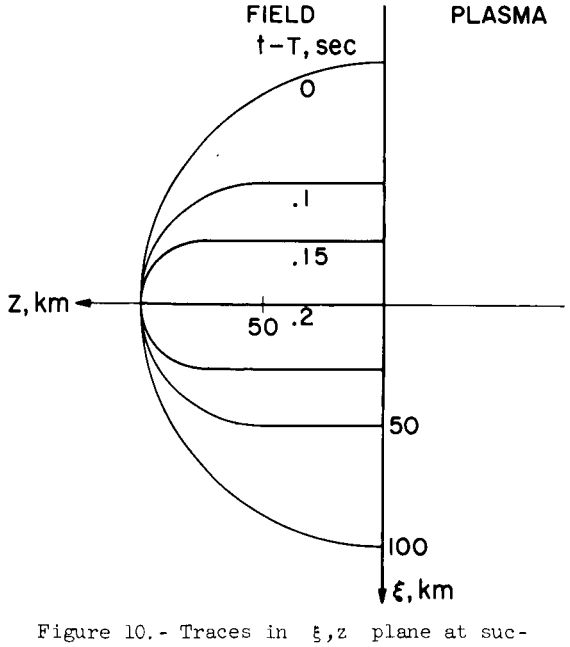

Figure 10.- Traces in ξ,z plane at successive times during late stages of collapse of dent in magnetosphere boundary.

Once a segment of the boundary becomes parallel to the z axis, it loses its ability to diminish the z component of the velocity of the incident particles. Whether considered

from the classical Chapman-Ferraro point of view in which the individual particles of the solar wind are specularly reflected from the boundary ($K = 2$ in eq. (3)), or from the more recently proposed point of view in which a fluid flows along the boundary ($K = 1$), particles encountering the straight segment of the boundary are merely shunted toward the opposite side of the dent as they continue their progress toward the circular nose of the dent. Although effects of a single particle experiencing multiple encounters with the boundary are not included in the foregoing analysis, it is evident that the number of particles, or the density of the fluid, confined within the dent increases with time as the dent collapses in width. As a result, the nose of the dent is subject to an additional pressure for a small interval of time immediately before the final collapse. This portion of the boundary will thereupon commence to move in the direction of the positive z axis, and it appears inevitable that a narrow column of compressed solar plasma will be injected in the magnetosphere. Its width will be a fraction of ϵ_o, and quite unrelated to the initial width of the dent. The time to collapse, however, depends very nearly on the square of the initial width, as indicated approximately by equation (71). Further analysis and discussion of the behavior of the dent and possible effects of double or multiple encounters is provided in the following section.

The actual magnetosphere boundary is not flat as assumed in this section, but curved. We have seen in the preceding section that curvature exerts a stabilizing or destabilizing influence on the boundary perturbations according to whether the center of curvature is on the field or plasma side of the boundary. For the former, equations (52) and (57) show that the amplitude of alined waves diminishes by a factor e in a time $t_{cur} = R/V_z$. It is of interest to compare this time with the time collapse t_{col} of a shallow circular dent of initial width W and amplitude ϵ_o. The ratio of these two times

$$\frac{t_{cur}}{t_{col}} = \frac{R/V_z}{W^2/2V_z\epsilon_o} = \frac{2\epsilon_o R}{W^2} \tag{74}$$

provides a measure of which tendency will tend to dominate. If t_{cur}/t_{col} is much greater than unity, the stabilizing effect of curvature will be small, and a dent will tend to collapse much as in the case described above for the flat equilibrium surface. If, on the other hand, this ratio is much less than unity, the collapsing action will have little time to develop and the stabilizing effect of curvature will dominate. If, for a numerical example, $R = 50{,}000$ km and $W = 1000$ km, then $t_{cur}/t_{col} = 1$ for $\epsilon_o = 10$ km. Thus, such dents will tend to smooth out with time if ϵ_o is substantially less than 10 km, and collapse with subsequent particle penetration if ϵ_o is substantially greater than 10 km. It would thus appear that even quite modest irregularities in the solar wind could result in isolated columns of solar plasma penetrating the boundary of the magnetosphere in spite of the stabilizing influence of curvature. The plasma in these columns would, moreover, retain its tangential momentum as it initially penetrates into the magnetosphere. Subsequent interaction with the ambient magnetosphere plasma would lead to a transfer of momentum across the boundary that might be roughly equivalent to the effective viscous interaction postulated in the

magnetosphere convection model of Axford and Hines (ref. 22). If, on the other hand, the solar wind is perfectly steady and free of irregularities, no penetration would occur, except in the vicinity of the neutral points where the boundary curvature reverses.

MOTION OF PARTICLES DURING FINAL STAGES OF COLLAPSE OF A CIRCULAR DENT IN THE MAGNETOSPHERE BOUNDARY

A critical point in the development of a semicircular cylindrical dent in the magnetosphere boundary is reached when the dent assumes such a form that a rebounding particle has positive rather than negative V_z. Since a particle with positive V_z will inevitably hit the boundary of the dent a second time, and add an effect not included in the foregoing analysis, it is of interest to inquire whether the dent reaches the semicircular form before the first double bounce occurs. If it does, the preceding discussion of the final stages of the collapse and possible injection of particles would have to be modified substantially. It is the object of this section to demonstrate, within the classical Chapman-Ferraro formulation of the problem with specular reflection at the boundary, that such double bounces do not occur before the dent becomes a semicircle. Double bounces do begin to occur slightly later, however, and the section is concluded with some quantitative remarks on the consequences thereof.

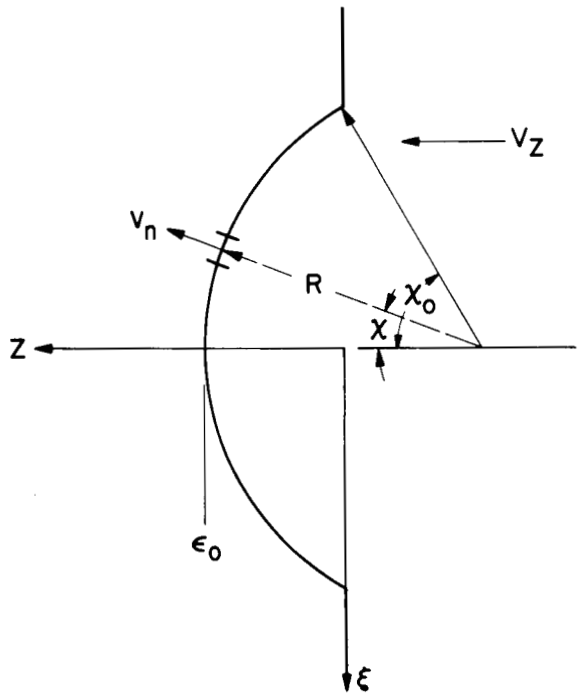

Figure 11.- View of trace in ξ,z plane of circular dent in magnetosphere boundary.

In a ξ,z coordinate system drifting along the boundary with the tangential component of the solar wind, and with the angles χ and χ_o and other quantities as illustrated in figure 11, equations (3) and (5) combine to yield the following expressions for the normal velocity v_n of a segment P of a circular dent

$$v_n/V_Z = -1 + \cos \chi \qquad (75)$$

Particles of the undisturbed incident solar plasma approach P with velocity components $V_{\perp_o}$ and $V_{\parallel_o}$ perpendicular and parallel the local surface element given by

$$V_{\perp_o} = V_Z \cos \chi , \qquad V_{\parallel_o} = V_Z \sin \chi \qquad (76)$$

Relative to P, which is itself moving with normal velocity v_n, the corresponding component velocities of the particle are

$$V_{\perp R_o} = V_z \cos \chi - v_n , \qquad V_{\parallel R_o} = V_z \sin \chi \tag{77}$$

Upon impact, the tangential velocity component remains unchanged, and the normal velocity component relative to P is reversed. Designating the velocity components after rebound by subscript 1, we have

$$V_{\perp R_1} = -V_z \cos \chi + v_n, \qquad V_{\parallel R_1} = V_z \sin \chi \tag{78}$$

Returning to the original ξ, z coordinate system, we have

$$V_{\perp_1} = -V_z \cos \chi + 2v_n = V_z(\cos \chi - 2) , \qquad V_{\parallel_1} = V_z \sin \chi \tag{79}$$

Resolution into components parallel to the ξ, z coordinate axes, that drift with the tangential component V_x of the solar wind, yields

$$V_{\xi_1} = -V_\perp \sin \chi + V_{\parallel_1} \cos \chi = 2V_z \sin \chi \tag{80a}$$

$$V_{z_1} = V_\perp \cos \chi + V_{\parallel_1} \sin \chi = V_z(1 - 2 \cos \chi) \tag{80b}$$

The resultant speed of the rebounding particles is thus (in the drifting coordinate system)

$$V_1 = (V_{\xi_1}^2 + V_{z_1}^2)^{1/2} = V_z(5 - 4 \cos \chi)^{1/2} \tag{81}$$

Equation (80b) shows that a particle that strikes the edge of the dent where $\chi = \chi_o$ rebounds exactly along the ξ axis with $V_{z_1} = 0$ if $\cos \chi_o = 1/2$. The critical value for χ_o is thus 60°. Equation (81) shows that the rebounding particle travels with velocity $\sqrt{3}V_z$ and arrives at the origin at exactly the same instant as the center of the dent, since the half width of the dent is $\sqrt{3}$ times the distance from the origin to the center of the circular arc defining the dent when $\chi_o = 60^\circ$ and the center is itself moving with velocity V_z. It is thus evident that this particle will not experience a double collision prior to the time at which the dent attains a semicircular form.

Since it is not immediately evident that the particle to which attention is directed in the preceding paragraph is the first to actually experience a double collision, it is important to inquire further and determine the coordinates, at the moment the dent becomes semicircular, of all the particles that hit the dent in all preceding time. To be precise, consider the location at $t = T$ of the particles that collided with any part of the dent at an earlier time t_c when the center of the dent is at

$$z_c = -V_z\Delta t \ , \qquad \xi_c = 0 \tag{82}$$

the radius R is

$$R = \epsilon_o + V_z\Delta t \tag{83}$$

and the angle χ_o is

$$\chi_o = \cos^{-1}(V_z\Delta t/R) \tag{84}$$

where $\Delta t = T - t_c$. The coordinates of an arbitrary point P at time t_c are

$$\xi_{P_c} = -R \sin \chi \tag{85a}$$

$$z_{P_c} = R(\cos \chi - \cos \chi_o) \tag{85b}$$

where, as always, $|\chi| \leq |\chi_o|$. Particles colliding with the dent at t_c thus travel for an interval of time Δt with velocity components given by equation (80) and arrive at the following coordinates at T.

$$\xi = \xi_{P_c} + V_{\xi_1}\Delta t = R \sin \chi(-1 + 2 \cos \chi_o) \tag{86a}$$

$$z = z_{P_c} + V_{z_1}\Delta t = R \cos \chi(1 - 2 \cos \chi_o) \tag{86b}$$

This result shows that these particles are situated on the portion of a circular arc of radius

$$(\xi^2 + z^2)^{1/2} = R\left|1 - 2 \cos \chi_o\right| = \epsilon_o\left|1 - \frac{V_z\Delta t}{\epsilon_o}\right| \tag{87}$$

that extends over the range of angles given by

$$|\chi| \leq |\chi_o| = \left|\cos^{-1}\frac{1}{1 + \epsilon_o/V_z\Delta t}\right| = \left|\cos^{-1}\frac{V_z\Delta t}{\epsilon_o + V_z\Delta t}\right| \tag{88}$$

The results are plotted in dimensionless form in figure 12. The various circular arcs define the location at $t = T$ of the particles that collided with the dent at such earlier times that the ratio $V_z\Delta t/\epsilon_o$ had the numerical value indicated. The final conclusion is that a circular dent in the magnetosphere boundary is able to collapse all the way to a semicircle before the first double bounce occurs.

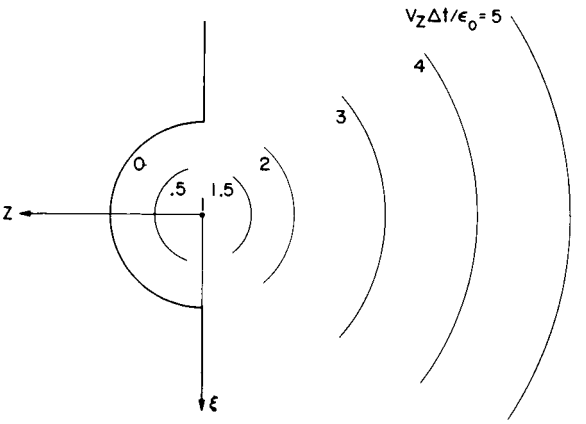

Figure 12.- Location at time T of particles that were specularly reflected from the dent at earlier time.

For a certain interval of time after the center of the circle passes the origin, the dent will continue to collapse without any double encounter with a particle. During this time, the nose of the dent will continue to be described by a semicircle as discussed previously and as illustrated in figure 12. The radius of the circular nose is $\epsilon_o - V_z(t - T)$, and the sides are parallel to the z axis. The flat sides of the dent are thus traveling toward the z axis with velocity equal to V_z, and particles encountering these surfaces will be deflected with a velocity component in the ξ direction equal to $\pm 2V_z$ while the component in the z direction remains unchanged and equal to V_z.

As demonstrated near the beginning of this section, the first particle that is deflected in such a way as to insure a double impact is the one that makes initial contact with the edge of the dent when $X_o = 60^\circ$. It is deflected so as to travel exactly along the ξ axis with velocity $\sqrt{3}V_z$, and hence passes through the origin at the same instant ($t = T$) as the center of the dent. This particle continues on its way, and makes its second encounter with the surface of the dent at the instant when the radius of the circle is equal to $\epsilon_o(3 - \sqrt{3})/2 \approx 0.63\epsilon_o$. The center of the circle is thus at about $0.37\epsilon_o$, and the configuration of the dent is as illustrated in figure 13. The additional pressure exerted on the boundary by these and succeeding particles will

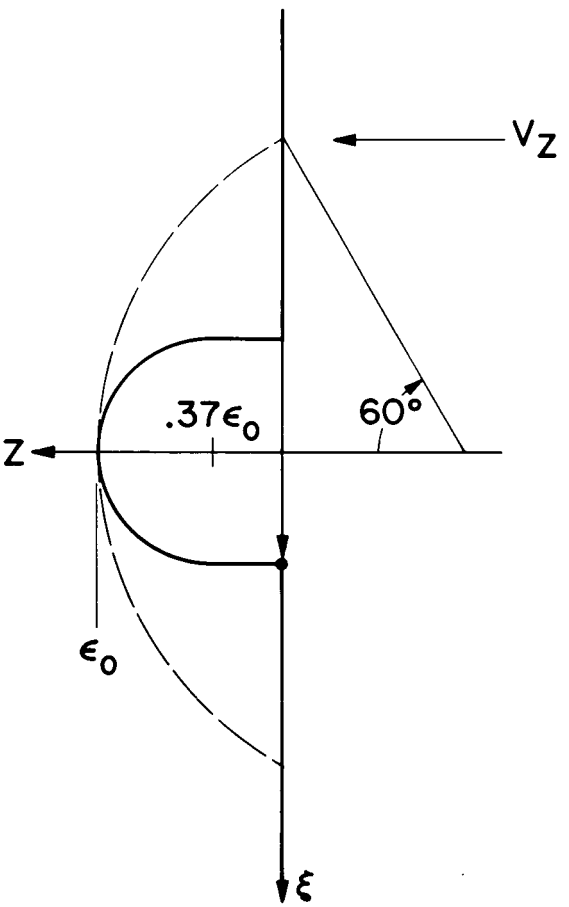

Figure 13.- Configuration of dent at instant when particle which was deflected from edge of the dent when $X_o = 60^\circ$ makes its second impact.

cause the portion of the flat surface nearest the axis to be slowed somewhat in its advance toward the z axis. This effect must be of a rather transient nature, however, because the initial deflection must occur after the time when $\chi_o = 60^o$, and the entire effect is terminated well before the time when $\chi_o = 90^o$. In any case, the total effect is expected to be too weak and transient to prevent this portion of the dent from continuing its advance toward the z axis until, eventually, the two sides meet and the original plane boundary of the geomagnetic field is restored along the ξ axis.

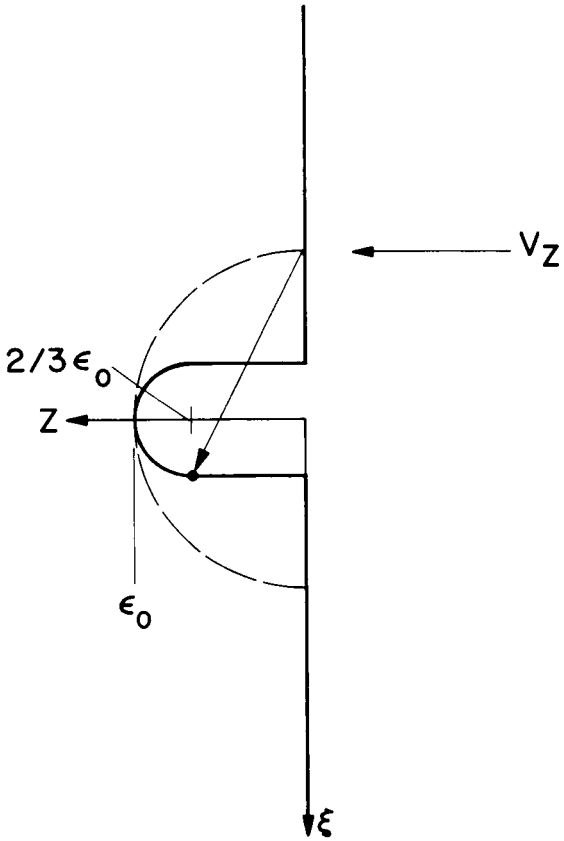

Figure 14.- Configuration of dent at instant when first particle to be deflected from the flat surface of the dent makes its second impact.

At a slightly later instant, when the center of the semicircle progresses to $2\epsilon_o/3$, the first particle to bounce off the flat surface will encounter the opposite side of the dent. It will hit at exactly the junction of the straight and circular elements, as illustrated in figure 14, and moreover, will be followed by a steady stream of particles extending over a steadily widening portion of the side of the dent. The particles approaching their second encounter with the dent in $x > 0$ have velocity components $\underline{V}_z = V_z$, $\underline{V}_x = 2V_z$, and number density $\underline{n} = n/2$ where n is the density in the undisturbed stream. Then equations (3) and (5) combine to yield the following expression for the velocity of the affected portion of the straight segment of the dent

$$B_{se}^2/8\pi = 2mnV_z^2 = 2m\underline{n}(\underline{V}_x - v_n)^2$$

$$= mn(2V_z - v_n)^2 \qquad (89)$$

Solving for v_n/V_z, we get

$$v_n/V_z = 2 - \sqrt{2} \approx 0.59 \qquad (90)$$

We thus find this portion of the dent bulging out into the magnetosphere at the same time as the portion of the dent near the ξ axis is snapping shut much in the manner illustrated in figure 15. This analysis supports the

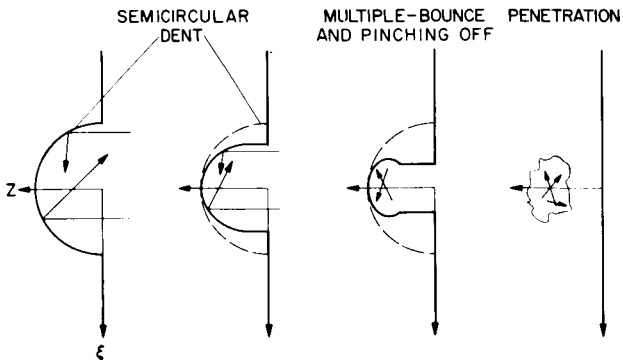

Figure 15.- Sketch of possible mechanism for injection of columns of solar wind plasma into magnetosphere.

more qualitative discussion provided in the preceding section, and lends support to the conclusion presented there that this mechanism appears capable of injecting widely separated columns of solar plasma into the magnetosphere under all but the steadiest of conditions.

Ames Research Center
National Aeronautics and Space Administration
Moffett Field, Calif., June 11, 1964

REFERENCES

1. Dungey, J. W.: Cosmic Electrodynamics. Cambridge University Press, Cambridge, 1958, pp. 151-152.

2. Dungey, J. W.: The Structure of the Exosphere or Adventures in Velocity Space. Geophysics, the Earth's Environment. C. DeWitt, J. Hieblot, and A. Lebeau, eds., Gordon and Breach, Science Publishers, New York, London, 1963, pp. 505-550.

3. Parker, E. N.: Interaction of the Solar Wind With the Geomagnetic Field. Phys. Fluids, vol. 1, 1958, pp. 171-187.

4. Hines, C. O.: The Magnetopause: A New Frontier in Space. Science, vol. 141, 1963, pp. 130-136.

5. Spreiter, John R.: The Boundary of the Geomagnetic Field. ICSU Review of World Science, vol. 6, 1964, pp. 178-190.

6. Chapman, Sydney: Solar Plasma, Geomagnetism and Aurora. Geophysics, the Earth's Environment. C. DeWitt, J. Hieblot, and A. Lebeau, eds., Gordon and Breach, Science Publishers, New York, London, 1963, pp. 373-502.

7. Dessler, A. J.: The Stability of the Interface Between the Solar Wind and the Geomagnetic Field. J. Geophys. Res., vol. 66, 1961, pp. 3587-3590.

8. Dessler, A. J.: Further Comments on Stability of Interface Between Solar Wind and Geomagnetic Field. J. Geophys. Res., vol. 67, 1962, pp. 4892-4894.

9. Coleman, P. J., Jr., and Sonett, C. P.: Note on Hydromagnetic Propagation and Geomagnetic Field Stability. J. Geophys. Res., vol. 66, 1961, pp. 3591-3592.

10. Barthel, J. R., and Sowle, D. H.: A Mechanism of Injection of Solar Plasma Into the Magnetosphere. Planetary and Space Science, vol. 12, 1964, pp. 209-217.

11. Spreiter, John R., and Alksne, Alberta Y.: On the Effect of a Ring Current on the Terminal Shape of the Geomagnetic Field. J. Geophys. Res., vol. 67, 1962, pp. 2193-2205.

12. Spreiter, John R., and Alksne, Alberta Y.: The Effect of a Ring Current on the Boundary of the Geomagnetic Field in a Steady Solar Wind. NASA TR R-177, 1963.

13. Spreiter, John R., and Briggs, Benjamin R.: Theoretical Determination of the Form of the Hollow Produced in the Solar Corpuscular Stream by Interaction With the Magnetic Dipole Field of the Earth. NASA TR R-120, 1961.

14. Spreiter, John R., and Briggs, Benjamin R.: Theoretical Determination of the Form of the Boundary of the Solar Corpuscular Stream Produced by Interaction With the Magnetic Dipole Field of the Earth. J. Geophys. Res., vol. 67, 1962, pp. 37-51.

15. Axford, W. I.: The Interaction Between the Solar Wind and the Earth's Magnetosphere. J. Geophys. Res., vol. 67, 1962, pp. 3791-3796.

16. Kellogg, P. J.: Flow of Plasma Around the Earth. J. Geophys. Res., vol. 67, 1962, pp. 3805-3811.

17. Spreiter, John R., and Jones, Wm. Prichard: On the Effect of a Weak Interplanetary Magnetic Field on the Interaction Between the Solar Wind and the Geomagnetic Field. J. Geophys. Res., vol. 68, 1963, pp. 3555-3564.

18. Ferraro, V. C. A.: On the Theory of the First Phase of a Geomagnetic Storm: A New Illustrative Calculation Based on an Idealized (Plane not Cylindrical) Model Field Distribution. J. Geophys. Res., vol. 57, 1952, pp. 15-49.

19. Beard, David B.: The Interaction of the Terrestrial Magnetic Field With the Solar Corpuscular Radiation. J. Geophys. Res., vol. 65, 1960, pp. 3559-3568.

20. Mead, Gilbert D.: Deformation of the Geomagnetic Field by the Solar Wind. J. Geophys. Res., vol. 69, 1964, pp. 1181-1195.

21. Fukushima, N.: Gross Character of Geomagnetic Disturbance During the International Geophysical Year and the Second Polar Year. Report of Ionosphere and Space Research in Japan, vol. 16, 1962, pp. 37-56.

22. Axford, W. I., and Hines, C. O.: A Unifying Theory of High-Latitude Geophysical Phenomena and Geomagnetic Storms. Canadian J. Phys., vol. 39, 1961, pp. 1433-1464.

NASA-Langley, 1965 A-995